Supporting Information

Bhadury et al. 10.1073/pnas.1406722111

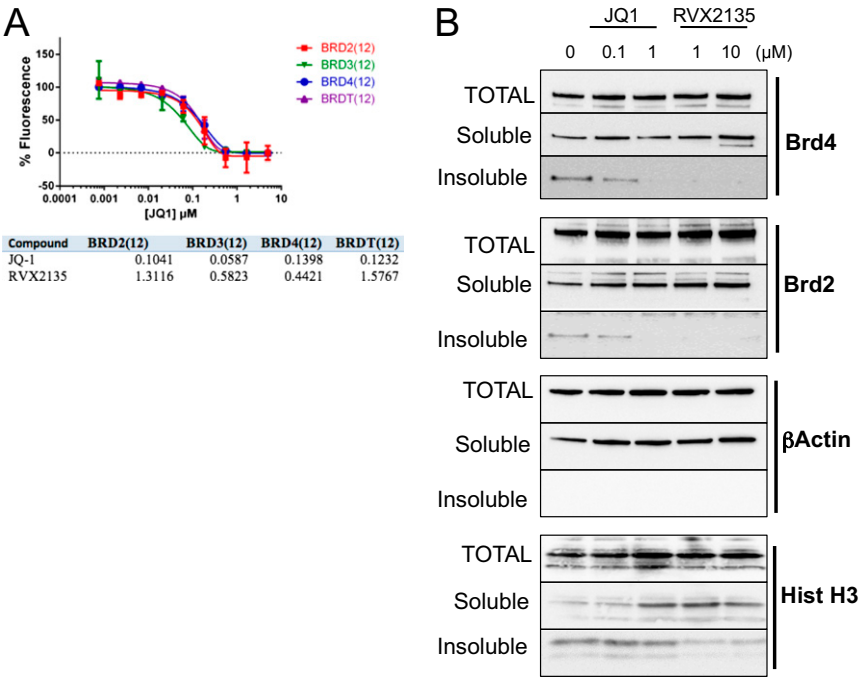

Compound	BRD2(12)	BRD3(12)	BRD4(12)	BRDT(12)
JQ-1	0.1041	0.0587	0.1398	0.1232
RVX2135	1.3116	0.5823	0.4421	1.5767

Fig. S1. Bromodomain and extraterminal inhibitors (BETi) displace BET proteins from acetylated histones in chromatin. (*A*) The same assay as in Fig. 1 was used to determine the IC_{50} of the prototype BETi JQ1. IC_{50} values (μM) for both BETi are shown in the table beneath the dose–response curve. Data are mean values ± SD (error bars). (*B*) BETi displace Brd2 and Brd4 from chromatin in λ820 cells. Cells were cultured in the presence of BETi or vehicle (DMSO) for 24 h. Cells were counted and an equal number of cells was pelleted in two different tubes per treatment. Five of the pellets (one per treatment) were used to make a total lysate, where the pellet was dislodged and then resuspended in a standard Western blot lysis buffer, sonicated with a tip sonicator, and boiled in SDS loading dye before being loaded on a gel. The remaining five pellets from the experiment were lysed on ice in a standard lysis buffer for Western blot and mildly sonicated using a Bioruptor (Diagenode). The lysates were centrifuged (5,000 × *g*) and the supernatant (soluble fraction) was saved and processed for Western blot analysis. The remaining pellets contained cell debris and chromatin and were further processed in a stronger lysis buffer containing urea and sonicated using a tip sonicator. This highly viscous fraction (insoluble fraction) was processed for Western blot. All of the three fractions (total, soluble, and insoluble) were run on an SDS/PAGE gel, transferred to a nitrocellulose membrane, and probed for the indicated proteins. Actin served as a control for the soluble and total fractions, whereas Histone H3 was present in all fractions.

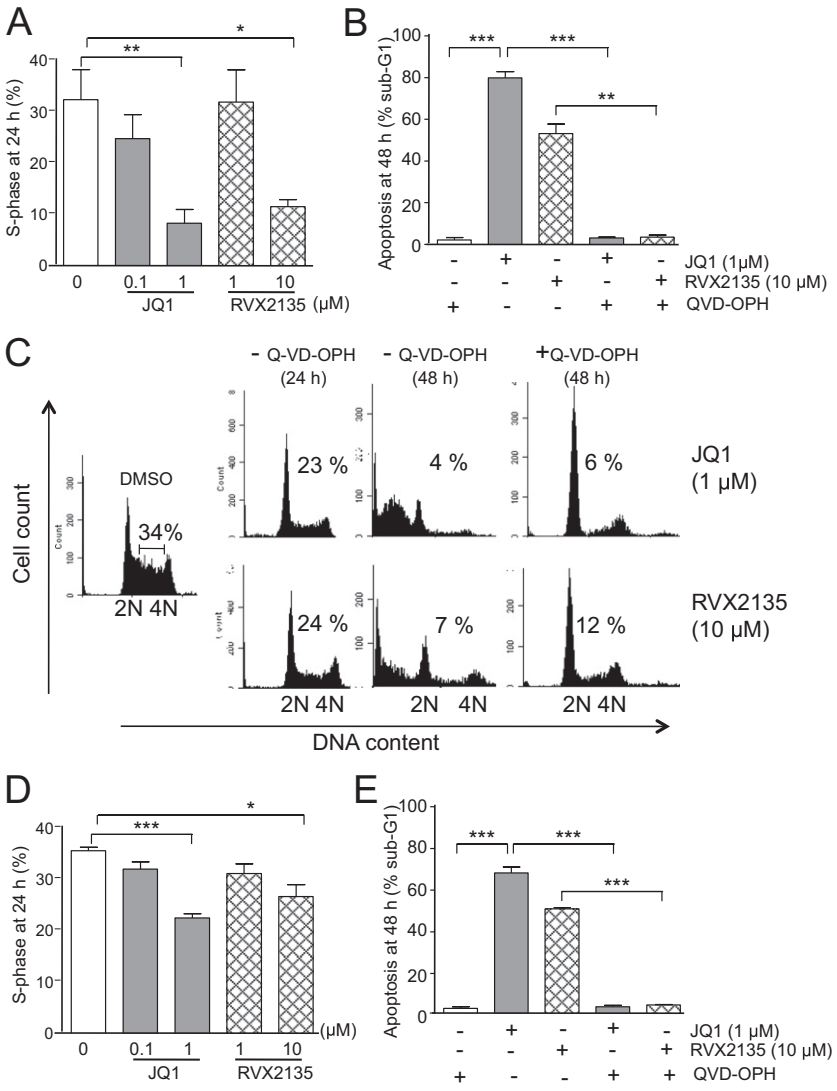

Fig. S2. λ820 cells were treated for 24 and 48 h with the indicated concentrations of BETi in the presence or absence of the pan-caspase inhibitor Q-VD-OPH. Cell-cycle distribution was analyzed by flow cytometry of 7-aminoactinomycin D (7-AAD)–stained cells. (*A* and *B*) Mean values of three independent experiments shown in Fig. 2*B*. (*C*) Same experiment in Eμ239 cells were performed; numbers show the proportion of cells in S phase (representative of three experiments). (*D* and *E*) Mean values of three independent experiments shown in *C*. Errors bars represent the standard deviation. $*P < 0.05$, $**P < 0.01$, $***P < 0.001$.

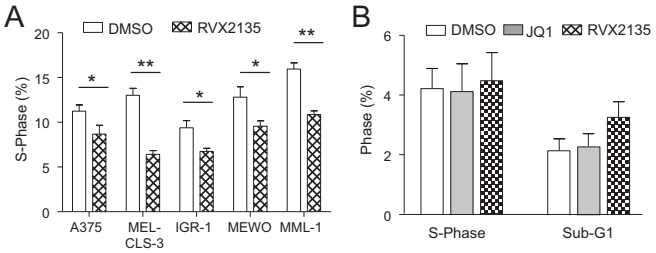

Fig. S3. Cells were treated for 48 h with BETi. Cell-cycle distribution was analyzed by flow cytometry of 7-AAD–stained nuclei. (*A*) Five melanoma cell lines were treated with 10 μM RVX2135. Representative mean values of two independent experiments run in biological triplicate. (*B*) Passage 2 mouse embryo fibroblasts were treated with vehicle (DMSO), 1 μM JQ1, or 10 μM RVX2135. Shown are mean values of two independent experiments run in triplicate. Errors bars represent the standard deviation. $*P < 0.05$, $**P < 0.01$.

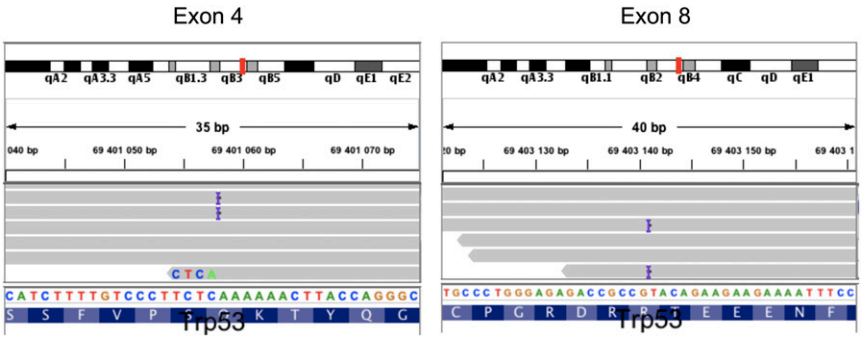

Fig. S4. Genomic DNA from λ820 cells was purified using the NucleoSpin Tissue DNA Kit (Macherey-Nagel). Exome sequencing was outsourced to Beijing Genomics Institute Hong Kong. Cleaned sequencing data were processed as recently described (1). Shown here are sequencing reads aligned in IGV tools v2. Two different insertion mutations that cause a frame-shift can be found in exons 4 and 8 of the *Trp53* gene in λ820 cells. The mutations result in an absence of mRNA expression and p53 protein expression (2), suggesting that the transcripts of the mutated *Trp53* alleles are targets of nonsense-mediated mRNA decay.

1. Bhadury J, López MD, Muralidharan SV, Nilsson LM, Nilsson JA (2013) Identification of tumorigenic and therapeutically actionable mutations in transplantable mouse tumor cells by exome sequencing. *Oncogenesis* 2:e44.
2. Höglund A, Nilsson LM, Forshell LP, Maclean KH, Nilsson JA (2009) Myc sensitizes p53-deficient cancer cells to the DNA-damaging effects of the DNA methyltransferase inhibitor decitabine. *Blood* 113(18):4281–4288.

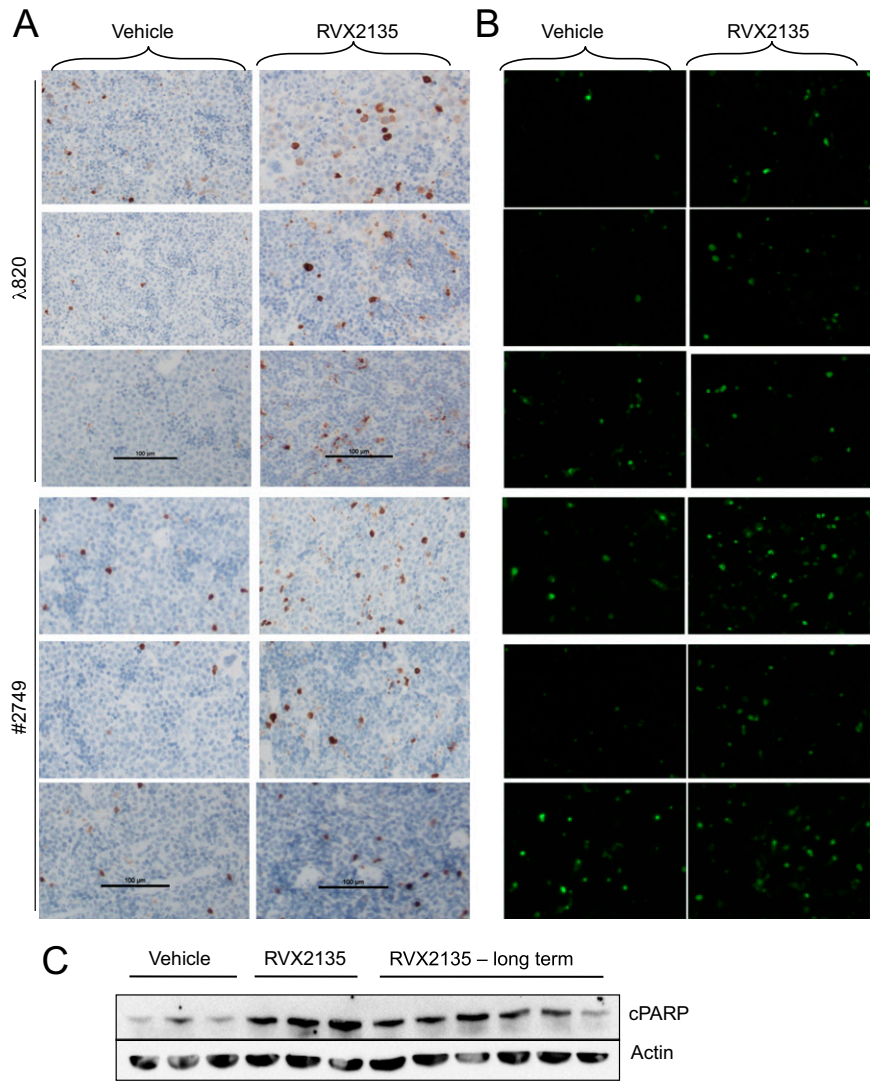

Fig. S5. (*A* and *B*) Immunohistochemistry (*A*) and TUNEL staining (*B*) of spleen sections from lymphoma-bearing mice treated with four (λ820) or five (2749) doses of vehicle or RVX2135 during 36 or 48 h before sacrifice. Shown are representative images of the sections quantified in Fig. 4 *A* and *B*. (*C*) Western blot analysis of cleaved PARP in lymph node tumors from acutely treated mice carrying λ820 tumors and mice treated in the survival curve in Fig. 3*A*. This experiment on acutely treated mice was performed twice with similar results.

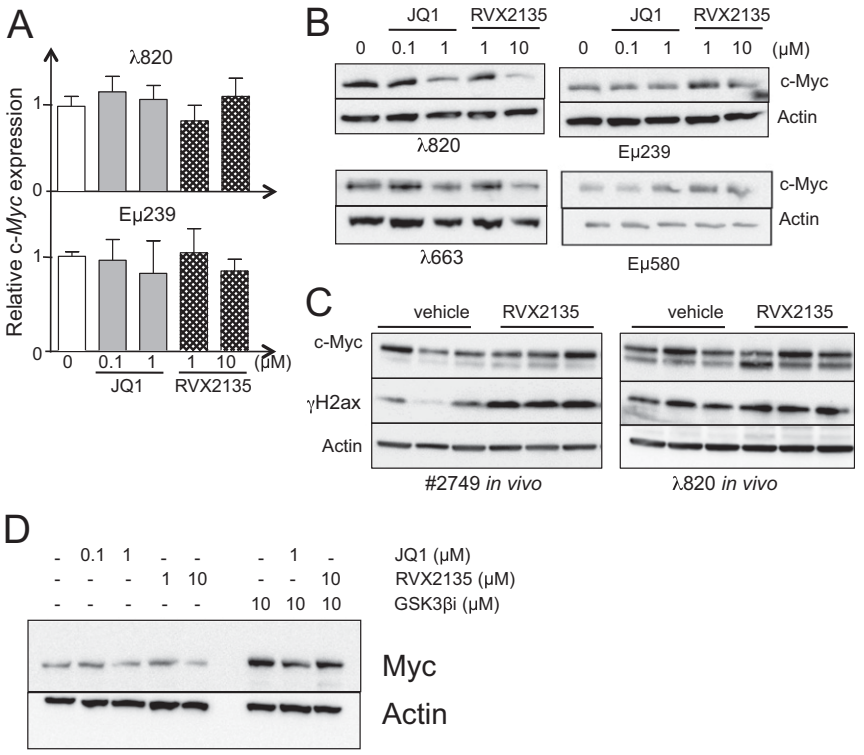

Fig. S6. BETi do not suppress Myc transcription in Myc-induced murine lymphoma cells. (*A*) Quantitative RT-PCR analysis of Myc RNA expression in the indicated cell lines treated with different concentrations of BETi. The data values are the mean expression of three independent experiments. (*B*) Western blot analysis of c-Myc protein levels in various murine lymphoma lines. (*C*) Western blot analysis of c-Myc protein and the DNA damage-induced phosphorylation of H2Ax (γH2Ax) in lymph node lymphomas from mice carrying the indicated cells and treated with RVX2135 or vehicle. (*D*) Western blot analysis of λ820 cells treated with the selective GSK3β inhibitor CHIR99021 (Selleck Chemicals) in the presence or absence of the indicated concentrations of BETi.

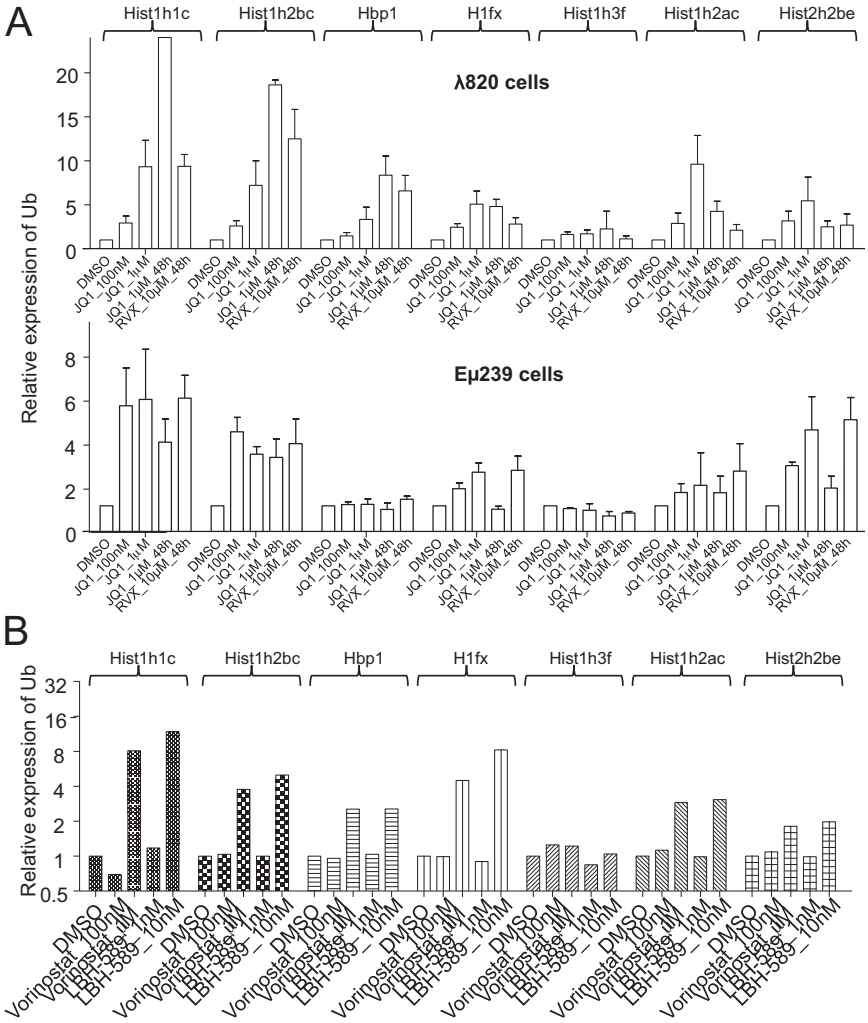

Fig. S7. (*A*) Quantitative RT-PCR analysis to confirm the regulation of histone mRNAs in λ820 and Eμ239 cells treated with the indicated concentrations of JQ1 or RVX2135 for 24 h (unless otherwise stated). Shown are mean values of three independent experiments. (*B*) Quantitative RT-PCR analysis to confirm the regulation of histone mRNAs in cells treated for 24 h with the indicated concentrations of vorinostat or LBH-589. Shown are one out of two independent experiments.

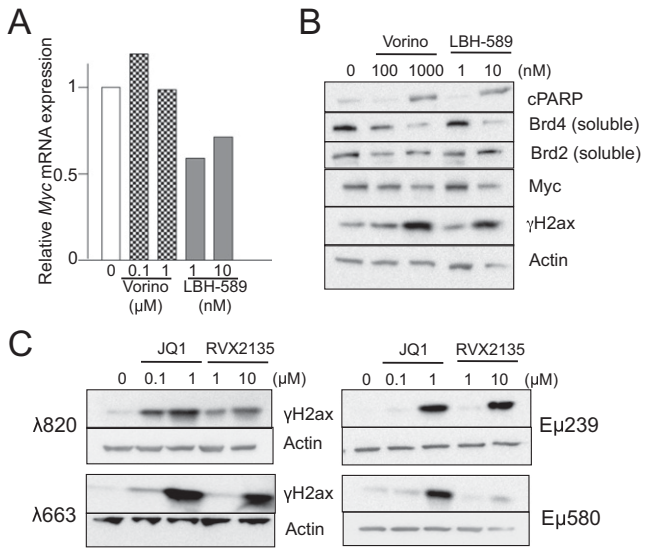

Fig. S8. BETi and histone deacetylase inhibitors (HDACi) induce similar phenotypes and synergistically kill Myc-induced lymphoma cells. (*A*) Quantitative RT-PCR analysis of Myc mRNA in λ820 cells treated for 24 h with the indicated concentrations of HDACi. (*B*) λ820 cells were treated for 24 and 48 h with the indicated concentrations of BETi. Cells were lysed and analyzed by Western blotting with the indicated antibodies. (*C*) Western blot analysis of histone 2Ax phosphorylation (γH2Ax) in the indicated lymphoma cell lines treated with increasing concentrations of BETi for 24 h.

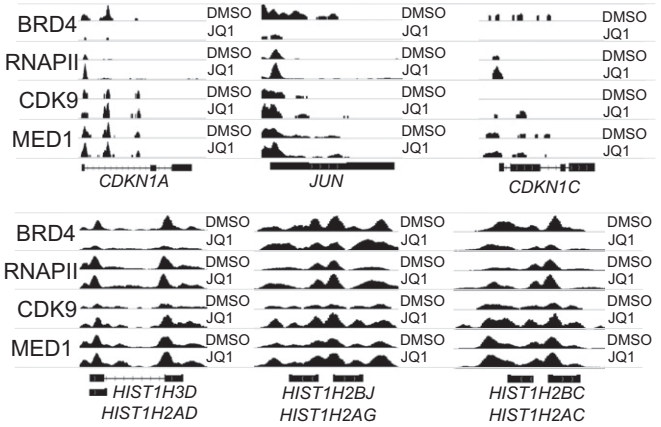

Fig. S9. BETi induce transcription in a Brd4-dependent and independent manner. Shown are IGV screenshots of different loci bound by the indicated proteins in ChIP-seq experiments performed in MM1.S cells (1). The selected genes are induced by BETi and/or HDACi in λ820 cells (Fig. 6*D*).

1. Lovén J,et al. (2012) Revisiting global gene expression analysis. *Cell* 151(3):476–482.

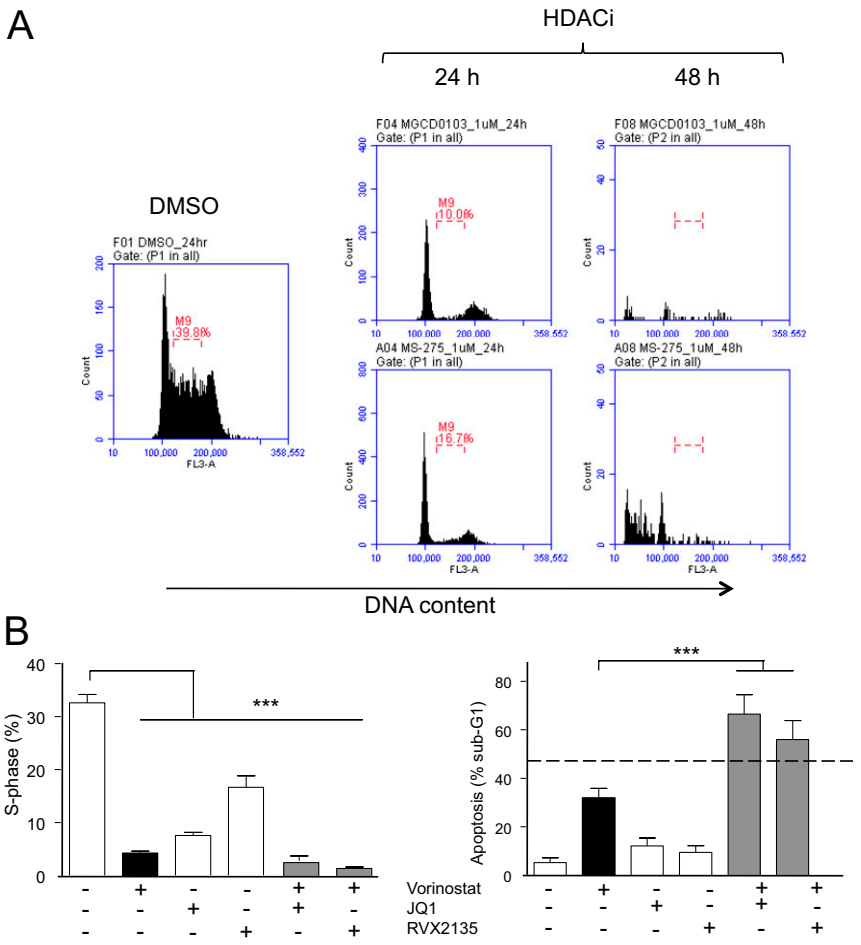

Fig. S10. (*A*) λ820 cells were treated with HDAC inhibitors MGCD0103 and MS-275 at 1 μM for 24 and 48 h. Shown are DNA histograms at concentrations where the cells arrested at 24 h and succumbed to cell death at 48 h. Graphs are representative of three independent experiments yielding the same results. (*B*) Quantification of data shown in Fig. 7*D*. λ820 cells were cultured in the absence or presence of 1 μM vorinostat, 1 μM JQ1, and/or 10 μM RVX2135 for 24 h. Cell-cycle distribution and apoptosis (sub-G1 DNA content) were determined by flow cytometry of nuclei stained with 7-AAD. Shown are mean values of three independent experiments. Apoptosis levels above the dashed line indicate more than additive levels. Errors bars represent the standard deviation. ***$P < 0.001$.

Other Supporting Information Files

Dataset S1 (XLSX)
Dataset S2 (XLSX)
Dataset S3 (XLSX)
Dataset S4 (XLSX)
Dataset S5 (XLSX)